07

Influence of oxygen vacancy concentration on the resistive switching parameters of $ZrO_2(Y)$-based memristor structures

© A.V. Kruglov, D.A. Serov, A.I. Belov, M.N. Koryazhkina, I.N. Antonov, S.Yu. Zubkov, R.N. Kriukov, D.A. Antonov, D.O. Filatov, V.A. Khabibulova, A.N. Mikhaylov, O.N. Gorshkov

Lobachevsky University of Nizhny Novgorod,
603022 Nizhny Novgorod, Russia
e-mail: krualex@yandex.ru

Received April 18, 2025
Revised July 7, 2025
Accepted July 11, 2025

The effect of oxygen vacancy concentration on the parameters of resistive switching in the memristors based on yttria stabilized zirconia $ZrO_2(Y)$ was studied. The concentration of oxygen vacancies inside the $ZrO_2(Y)$ film and in the region of resistive switching (metal/dielectric interface) varied by changing the doping impurity concentration (8 or 12 mol.% Y_2O_3) as well as by changing the oxygen exchange conditions by using different active electrode materials having different oxidation properties (Ta, W, or Ru). X-ray photoelectron spectroscopy and conductive atomic force microscopy have revealed the presence of a region saturated with oxygen vacancies and the formation of conductive channels during the manufacture of the memristor stacks that makes it possible to create the memristors, which do not require forming. Electrical measurements have shown that the stacks based on $ZrO_2(Y)$ films with the Y_2O_3 concentration of 8 mol.% demonstrated gradual resistive switching, smaller current state spread, and may be interesting for neuromorphic applications. The stacks with Ta and W electrodes demonstrated similar resistive switching parameters and good CMOS integration capabilities, while the stacks with Ru electrodes demonstrated the parameters incompatible with CMOS requirements.

Keywords: memristor, resistive memory, resistive switching, filament, current-voltage curve, electroforming, yttria-stabilized zirconia.

DOI: 10.61011/TP.2025.09.61846.71-25

Introduction

Memristors are considered promising candidates to be applied in a nonvolatile computer memory and neuromorphic computing devices [1,2]. Despite significant progress in their research in recent years [3,4], there are only few studies dedicated to memristors that are integrated with complementary symmetry metal-oxide-semiconductor (CMOS) structures and demonstrate high indicators of resistance and stability of multiple resistive switching (RS) [5,6].

It is believed that wide practical introduction of the memristors is prevented by a significant spread of switching parameters, which has a fundamental origin, i.e. a stochastic nature of processes in its base. In the most cases, in the memristors based on oxide films (Oxide-based Resistive Random Access Memory, OxRRAM) [7,8] resistive switching is based on electrochemical reactions of oxidation and reduction of a dielectric thin film, which are localized in the area of one or more conducting channels (filaments) [9]. Switching between the various resistive states of the memristor occurs as a result of initial formation (across the entire thickness of the dielectric film (with subsequent destruction/restoration)) of a nanoscale filament with relatively high electron conductivity due to high concentration of defects in its composition. Usually, these defects in OxRRAM are intrinsic defects of the dielectric film, which are oxygen vacancies [10]. Resistive switchings of the memristor are realized as a result of a transition from the High Resistance State (HRS) into the Low Resistance State (LRS), i.e. the so-called SET-process and vice versa - from LRS into HRS, i.e. the so-called RESET process. The RS process includes cyclic restructuring of the filament's vacancy structure within the area of an interface with an electrode made of a chemically active metal, which occupies a volume of several cubic nanometers [11,12], while during the switching process a countable number of the vacancies is moved. At the same time, a flip of the oxygen ion to an adjacent vacancy changes the filament structure and, respectively, its electron conductivity. Thus, the concentration of the oxygen vacancies determines a value of the electron current and other RS parameters.

One of the widespread methods of improving resistance and stability of resistive switching is selection of optimal materials of the dielectric and the electrodes. One of the promising dielectrics that are considered as an insulator material is yttrium-stabilized zirconium dioxide $ZrO_2(Y)$ [13–15], which is related to the fact that a value of the concentration of the oxygen vacancies can be controlled by varying the concentration of the Y_2O_3 dopant [16]. When adding Y_2O_3 to ZrO_2, the Y^{3+} ions replace the Zr^{4+} ions. At the same time, the oxygen vacancies originate to ensure electrical neutrality of a crystal and a process of their formation can be described as an equation of the quasi-chemical reaction (in accordance with Kroeger-Wink

designations):

$$Y_2O_3 \xrightarrow{2ZrO_2} 2Y'_{Zr} + 3O^x_O + V^{\cdot\cdot}_O.$$

Thus, two Y^{3+} ions in the cation sublattice create one positively-charged vacancy in the anion sublattice ($V^{\cdot\cdot}_O$). Origination of additional vacancies promotes ion conductivity of $ZrO_2(Y)$. It should be noted [17,18] that at the higher temperature, with increase of the dopant concentration ion conductivity increases only in a small area of the concentrations of Y_2O_3 (3–9 mol.%), while at the high concentrations of Y_2O_3 (9–20 mol.%) conductivity decreases. Increase of the dopant content results in increase of a number of the oxygen vacancies, thereby facilitating diffusion of the O^{2-} ions. But further increase results in formation of associates of the vacancies with the Y^{3+} ions [19–22], which, in turn, complicates diffusion of the O^{2-} ions and, respectively, decreases ion conductivity. The literature has no data about the dependence of ion conductivity of $ZrO_2(Y)$ at the room temperature and at the temperatures that are typical for magnetron deposition of layers of memristor stacks.

High mobility of the oxygen ions is related to relatively small energy of formation of the active (mobile) oxygen vacancy (as compared to other oxides) (0.6 eV in ZrO_2 (12.5 mol.% Y_2O_3) [20]) as well as low energy of activation of migration of the oxygen ions along the oxygen vacancies (0.58–0.65 eV in ZrO_2 (12 mol.%Y_2O_3) [23,24]). Meanwhile, the effect of vacancy concentration on the resistive switching parameters in this material is still unstudied.

It should be noted that an alternative method of affecting the concentration and dynamics of the vacancies within the area of the metal/dielectric interface and, consequently, the resistive switching parameters is to vary oxygen exchange by using reactivity-different electrode materials. The experimental results [11,25–28] indicate an active role of the electrode material in the resistive switching process in the OxRRAM devices. Oxygen exchange reactions occur both during initial formation of the filament (an electroforming process) and the resistive switching process in each cycle. Meanwhile, it is essentially required that the electrode can oxidize in the SET process and reduce in the RESET process. The paper [25] has shown that dynamics of oxygen exchange with the dielectric is affected by reactivity of a metal, which is characterized by a standard oxide formation Gibbs energy ($\Delta_f G^o$). Stabilization of resistive switching (reduction of the spread of the resistive switching parameters) and increase of resistance to multiple resistive switchings require selection of the materials of the dielectric film and the electrode, which have similar values of the Gibbs energy. It is optimal when processes of oxidation and donation of oxygen by the metal are equally probable in the process of cyclic switchings. Then resistive switchings occur at relatively low voltages (compatible with CMOS-logic levels) with the least spread of the values of voltages and currents [11,26]. Therefore, an experimental study of a combination of $ZrO_2(Y)$ with various materials of the electrodes is of high practical interest. Thus, achievement of the best resistive switchings parameters and successful integration of the memristors into a CMOS technological process are possible due to optimal selection of the materials and engineering of the interfaces in their structure.

The present paper presents results of experimental study of the effect of oxygen vacancy concentration on the resistive switching parameters in the $ZrO_2(Y)$-based memristor stacks, which has been done by means of X-ray photoelectron spectroscopy (XPS), conducting atomic-force microscopy (AFM) and electrophysical measurements. The value of oxygen vacancy concentration in a resistive switching area is changed by varying the concentration of the dopant (12 or 8 mol.% Y_2O_3) or changing oxygen exchange due to using different electrode materials (Ta, W, Ru).

1. Materials and methods

The research objects were stacks Pt(20 nm)/Me(40 nm)/$ZrO_2(Y)$(20 nm)/Pt(40 nm). Ta, W or Ru were used as chemically active electrodes (Me). The stacks were formed on the oxidized silicon substrates SiO_2/Si that were metallized by the TiN/Ti layers. The Torr International 2G1-1G2-EB4-TH1 thin film deposition vacuum system was used to form the multilayer memristor stacks. The $ZrO_2(Y)$ films were deposited by high-frequency magnetron sputtering at the substrate temperature of 250 °C. The $ZrO_2(Y)$ films were applied using targets compressed from a mixture of the powders ZrO_2 and Y_2O_3 (88 mol.% / 12 mol.%–ZrO_2(12Y) or 92 mol.% / 8 mol.%–ZrO_2(8Y)). The lower electrodes (Pt) as well as the upper electrodes (Ta, W, Ru) with a protective layer (Pt) were applied by direct-current magnetron sputtering at the temperature of 200 °C. For the electrophysical measurements, the upper round electrodes of the diameter of about 100 μm with the protective layer Pt were formed through a shadow mask. Stacks with continuous layers of the upper electrode and the protective electrode were made for the XPS studies.

The electrophysical measurements of the stacks were carried out using the Agilent B1500A semiconductor device parameters analyzes using the EverBeing EB-6 probe station. The voltage sign on the stacks corresponded to a potential of the upper Me (Ta, W or Ru) electrode relative to a potential of the lower (Pt) electrode. The compliance current (I_{CC}) was limited using the Agilent B1500A software.

The composition of the memristor stacks was analyzed by the XPS method using the Multiprobe RM system (Omicron Nanotechnology GmbH, Germany). The layer-by-layer profiled was carried out by etching with Ar^+ ions at the energy of 1 keV. The following photoelectron lines were recorded — O 1s, C 1s, Zr 3d, Y 3d, Pt 4f, Ta 4f, W 4f. Since carbon is only in a thin subsurface area and is of no interest in the present study, the line C 1s is not shown in the figures. The maximum detectable concentration of the elements was 0.5 at.%. An error of determination of the

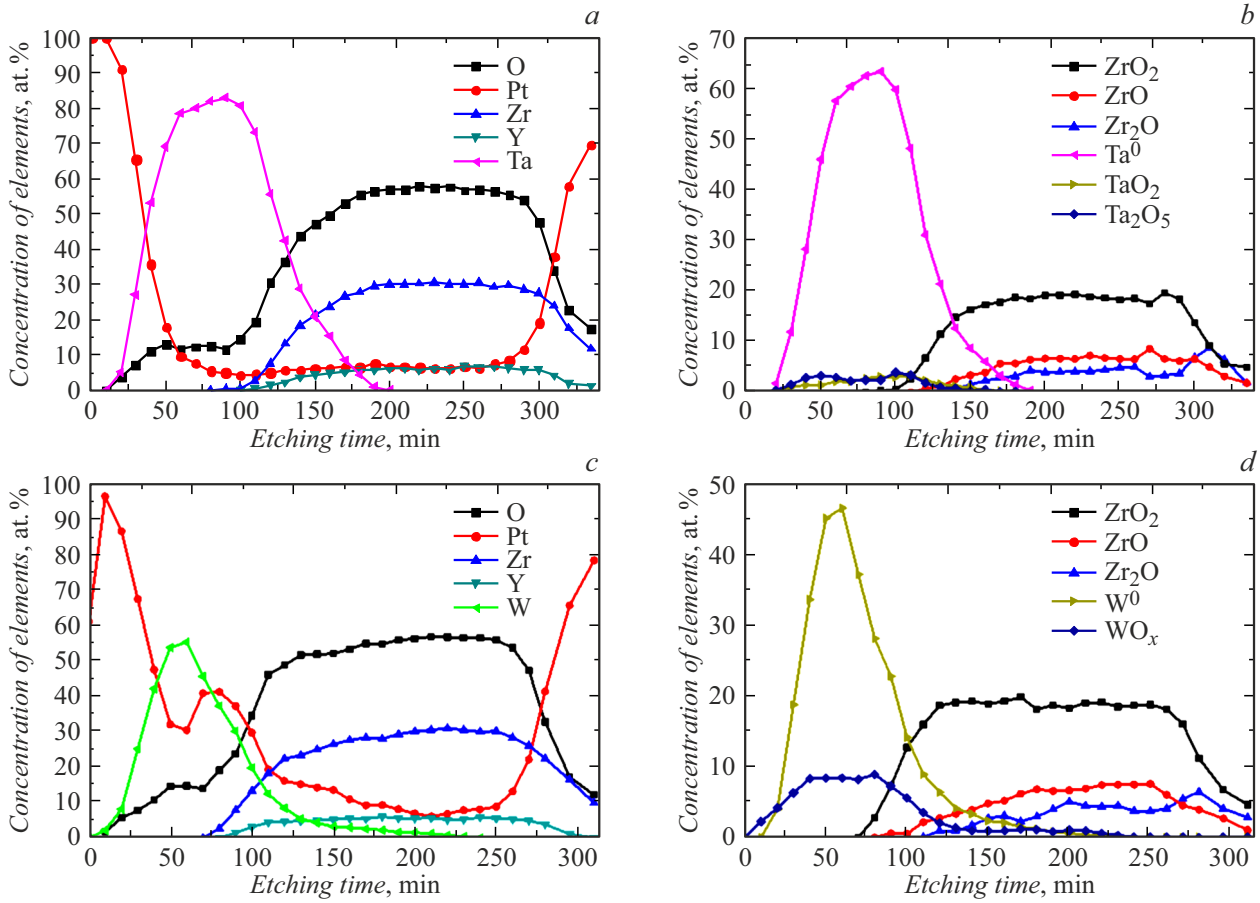

Figure 1. Profiles of distribution of concentration of the elements (*a*, *c*) and the chemical compounds (*b*, *d*) in a dependence on the etching time of the $ZrO_2(8Y)$-based stacks with the upper electrodes made of Ta (*a*, *b*) or W (*c*, *d*), which are obtained in layer-by-layer analysis by the XPS method.

depth did not exceed 2–3 nm. See the papers [29–31] for a more detailed description of the technique.

The initial state of the memristor stacks after ion off-etching of the upper metal electrode was studied using the conducting AFM method [32–34]. A morphology of the sample surface and a spreading resistance images were studied by means of a Ntegra Prima AFM produced by „NT-MDT“ (Zelenograd, Russia). The measurements were carried out using the probes ETALON HA_HR_DCP with a conducting diamond coating and a tip curvature radius of $\sim$ 100 nm.

2. Results and discussion

2.1. Results of the XPS studies

In the present study, the XPS method was taken to investigate the composition of the $ZrO_2(8Y)$-based stacks with the upper electrodes made of different chemically active metals (Ta, W). The results are shown in Fig. 1. In both the stacks, the active metal electrode is partially oxidized — a oxidation degree of the Ta electrode was about 12 at.%, and that of the W electrode was $\sim$ 14 at.%. Thus, when the electrode is deposited, the oxygen ions transit from an oxide layer near the interface into the electrode material to oxide it, while the oxygen vacancies remain at a location of the ions that passed from the oxide into the metal.

Previously, it was also shown by the XPS method in the paper [15] that when the memristor stacks were formed by magnetron sputtering the Ta electrode in contact with $ZrO_2(12Y)$ is oxidized (up to $\sim$ 27 at.%). By comparing the XPS results obtained from the stacks with the Ta electrode and the dielectric $ZrO_2(8Y)$ (Fig. 1, *a*) and $ZrO_2(12Y)$ [15], it can be noted that decrease of a doping degree from 12 to 8 mol.% results in reduction of the oxidation degree of the Ta electrode (from 27 at.% to 12 at.%). It can be related to reduction of mobility of oxygen ions along the oxygen vacancies due to their smaller concentration in the stack with the lower content of Y ($3.1 \cdot 10^{21}$ cm^{-3} and $2.1 \cdot 10^{21}$ cm^{-3} respectively in the stacks with 12 and 8 mol.% of Y_2O_3).

Results of chemical analysis demonstrate that the Ta layer has elementary Ta^0 and the compounds TaO_2 and Ta_2O_5

(Fig. 1, *b*). It is known that unlike the Ta_2O_5 dielectric phase [36,37] the TaO_2 phase is conducting [35]. In both the stacks (ZrO_2(8Y) and ZrO_2(12Y)) the tantalum amount in the Ta_2O_5 dielectric phase is approximately the same (4 at.%). The metal amount in the TaO_2 conducting phase in the stack with ZrO_2(12Y) [15] turned out to be in 4 times more than in the case of the stack with ZrO_2(8Y) (12 at.% and 3 at.%, respectively).

It should be noted that the W electrode (Fig. 1, *c*, *d*) as well as the Ta electrode is partially oxidized (there are W^0 and W_2O_3), but with a large amount of the oxidized metal ($\sim$ 14 at.%). This result is of applied importance, as, based on the values of standard free energy of formation of the metal oxides (see Table) it could be expected that the W electrode would be oxidized in a lesser degree than in the case with the Ta electrode.

This difference can be explained by the following circumstances. First of all, the tabular values of the Gibbs energy are known only for a limited set of oxides — for our used metals there are data for WO_2 and Ta_2O_5, whereas the experiment has exhibited formation of W_2O_3, Ta_2O_5 and TaO_2. It can be expected that the values of $\Delta_f G^o$ for W_2O_3 and TaO_2 significantly differ from those for WO_2 and Ta_2O_5. Secondly, the tabular values of $\Delta_f G^o$ are obtained for bulk materials, whereas the studies are carried out on nanoscale metal films that are formed by magnetron sputtering and subsequently oxidized due to oxygen exchange with ZrO_2(Y).

The XPS data also indicate diffusion of atoms of the protective layer (Pt) and the active electrodes (Ta, W) inward an insulating layer of the memristor stack. It is known [39] that the atoms of the electrodes can diffuse through the oxide layer in the memristor stack. It can result in formation of conductivity channels along metal bonds and, consequently, a mixed nature of conductivity (jump conductivity along the vacancies and metal conductivity along the metal bonds). However, current-voltage curves of the stacks with the Ta and W electrodes have been analyzed herein to show no specific features of resistive switching, which were related to the metal nature of conductivity.

2.2. Results of the study by the conducting AFM method

Results of determination of the initial resistive state of the memristor stacks have shown that they could be both in a non-conducting state and a conducting state [15]. The stacks based on the dielectric with the high content of the oxygen vacancies (12 mol.% of Y_2O_3) demonstrated the initial conducting state with low resistance, thereby making it possible to create memristors that do not require forming. It was assumed in the work [15] that the stacks had the initial conducting state since the insulator film had conducting channels that were generated during formation of the stacks, along which electron conductivity was realized.

The present study includes investigation by the conducting AFM method in order to establish the presence of such conducting channels. For this purpose, before investigation, the upper electrode with the protective layer (Pt/Ta) was removed from the stack Pt/Ta/ZrO_2(8Y)/Pt by an ion etching methods An off-etching depth was controlled by the XPS method by a signal from Zr and Ta as well as by the AFM method by a height of a step formed as a result of off-etching.

The conducting AFM probe was placed in two areas on the surface of the ZrO_2(8Y) film (Fig. 2, *a*): in the area 1, which initially had no upper electrode, and in the area 2 under the off-etched upper electrode. The AFM probe was grounded and the lower electrode (Pt) of the studied structure was energized voltage within $\pm$10 V.

In the area 1, the current image was uniform and the signal value did not exceed the noise level (0.2 nA) up to the voltages $\pm$10 V (Fig. 2, *b*). In the area 2, when applying the read-out voltage $\pm$0.15 V, there were many round current spots of the maximum diameter of about 100 nm and the current amplitude of up to 19 nA (Fig. 2, *c*), which we relate to current channels formed along grain boundaries in the dielectric. A study previously performed by us by the high-resolution TEM method [40] has shown that the ZrO_2 layers with 12 mol.% of Y_2O_3 grown by high-frequency magnetron sputtering in similar conditions had a polycrystalline structure and were in a cubic phase. Grains of the size $\sim 10-20$ nm are oriented perpendicular to planes of the electrodes. At the same time, it is well known that it is grain boundaries that are paths of predominant formation of the conducting filaments [41–43]. However, it is impossible to unambiguously compare a position of the current channels with specific features (grain boundaries) on the image of the surface morphology due to a large ($\sim$ 100 nm) rounding radius of the used conducting probe.

It was also found that during the second scanning of the same area the value of the current signal was reduced up to complete disappearance (Fig. 3). Thus, at the probe radius of 100 nm even small applied voltage (0.15 V) results in formation of the conducting channel (generated during manufacturing of the stacks) due to displacement (dissipation) of the oxygen vacancies under effect of the electric field.

The current images of the small size ($1 \times 1\,\mu$m) clearly exhibited asymmetry of current contrast (Fig. 3, *a*) that consisted in the fact that the spots of increased conductivity were horizontally extended (along a direction of fast AFM scanning). It is assumed that this specific feature is related to the above-said destruction of the initial conducting channels when scanning the sample surface.

2.3. Results of electrophysical measurements

Fig. 4 shows current-voltage curves (CVC) of memristor structures based on ZrO_2(12Y) and ZrO_2(8Y) with Ta-electrode, measured at the same value of the clamping current (I_{CC}). Minimum value of I_{CC}, when the structures based on ZrO_2(8Y) demonstrate RS, was equal to 500 μA, and RS in case of the structures based on ZrO_2(12Y) may

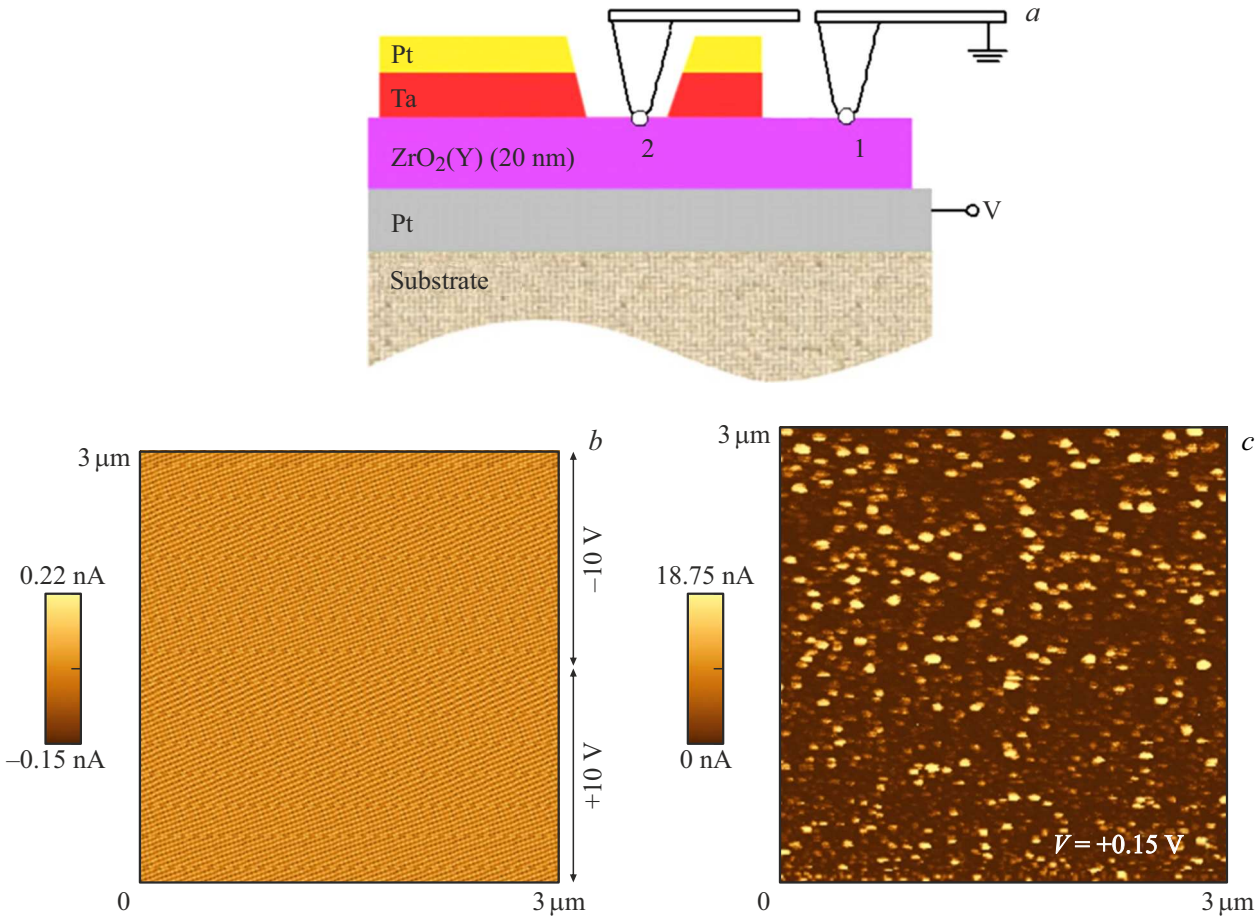

Figure 2. Diagram of investigation of the initial resistive state of the memristor stacks by the conducting AFM methods within the area 1, which initially had no upper electrode, and within the area 2 under the off-etched upper electrode (a). Current images of the surface of the $ZrO_2(8Y)$ film within the area 1 (b), as obtained under voltage of ± 10 V, and within the area 2 (c), as obtained under read-out voltage of $+0.15$ V.

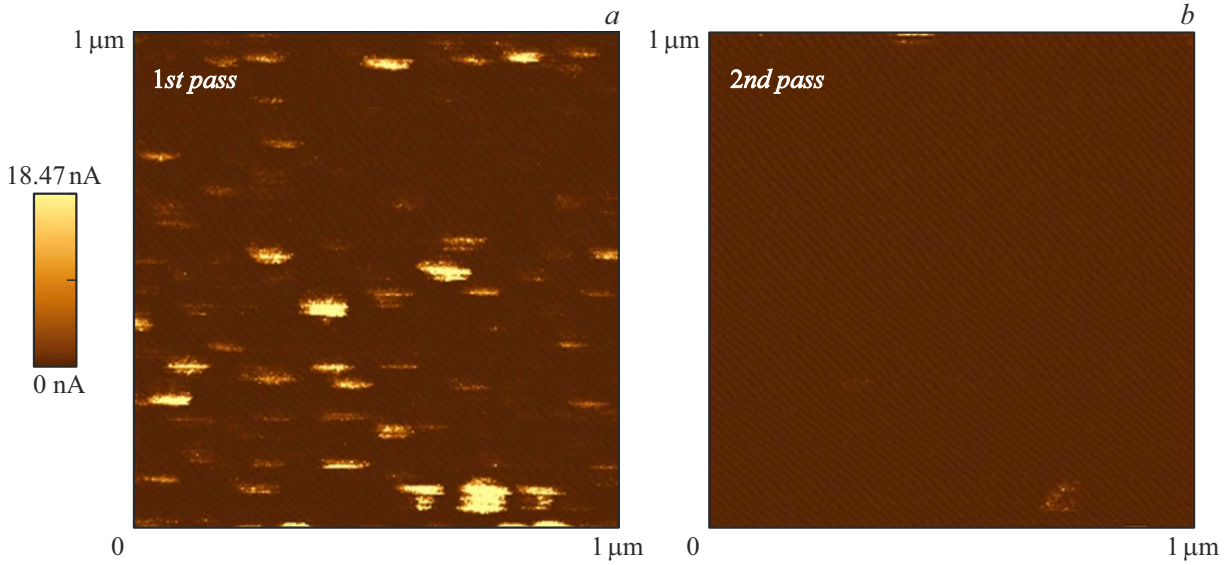

Figure 3. Current images of the surface of the $ZrO_2(8Y)$ film within the area 2, as obtained in the first (a) and the second (b) scanning. The images are obtained at the read-out voltage of $+0.15$ V.

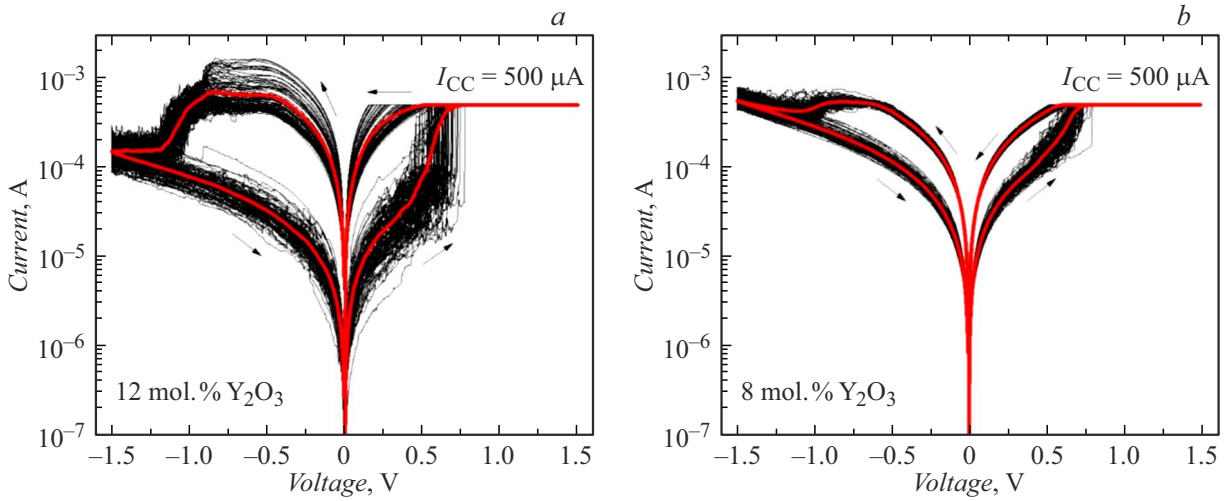

Figure 4. Typical current-voltage curves of the $ZrO_2(Y)$-based stacks with Ta electrode at the various concentration of the Y_2O_3 dopant: 12 mol.% (*a*) and 8 mol.% (*b*). The graphs show series of 100 current-voltage curves (in black) and the averaged curves (in red).

be implemented at lower values of I_{CC} [15]. It is assumed that such difference is related to lower concentration of oxygen vacancies necessary to develop the conducting filament in the structures based on $ZrO_2(8Y)$. It is also found that in case of the $ZrO_2(12Y)$-based stacks sharper resistive switchings are realized, whereas it is not always possible to determine voltages of the SET process (V_{SET}) and the RESET process (V_{RESET}) for the $ZrO_2(8Y)$-based stacks due to smoothness of the resistive switching process. It is assumed that in case of the $ZrO_2(12Y)$-based stacks, filaments with the higher current-carrying capacity are formed due to higher concentration of the oxygen vacancies (i.e. with the stack that is more saturated with the oxygen vacancies). This, in turn, can determine the nature of resistive switching.

Fig. 5 shows results of statistical processing of the series of the current-voltage curves shown in Fig. 4, namely, cumulative distribution functions of current states of the memristor, which are calculated at the read-out voltage of +0.15 V. It is found that in case of the $ZrO_2(8Y)$-based stacks there is a significantly lower spread of the current states. At the same time, one should not a difference in the value of the currents in LRS (I_{LRS}) and HRS (I_{HRS}) — the $ZrO_2(8Y)$-based stacks demonstrate a lower value of I_{LRS} and a higher value of I_{HRS} and, respectively, the smaller difference in the ratio of these currents (I_{LRS}/I_{HRS}) — on average, this ratio is 4.4 in case of the $ZrO_2(8Y)$-based stacks and 11 in case of the $ZrO_2(12Y)$-based stacks.

The difference in the obtained results for the $ZrO_2(Y)$-based stacks with the different concentration of the dopant can be related to several circumstances. As said above, in case of the $ZrO_2(12Y)$-based stacks, the large concentration of the oxygen vacancies as caused by higher equilibrium concentration of the vacancies due to yttrium doping and higher local concentration of the vacancies near the active electrode due to a higher oxidation degree of the Ta electrode can result in formation of the filaments that are more saturated with the oxygen vacancies. Therefore, electron conductivity and, respectively, a value of the current in the current-voltage curve in LRS have higher values in case of the $ZrO_2(12Y)$-based stacks.

The large spread of the current states in case of the $ZrO_2(12Y)$-based stacks can be related to the Current Overshoot Effect [44], which is observed when $I_{CC} = 500\,\mu$A (Fig. 4, *a*). This effect means that physically a current limitation unit (of a software or general-circuit type) has not enough time to limit the current that flows through the memristor in the SET process. Consequently, the current in LRS has a higher spread, which, in turn, results in increase of the current spread in HRS, as the same voltage sweep results in switching from the more conducting LRS into the more conducting HRS and, vice versa, from the less conducting LRS into the less conducting HRS.

Alternative explanation of the spread of the current states can be related to a different crystal structure of the stabilized zirconium dioxide films. It is known that $ZrO_2(12Y)$ at the room temperature has a cubic phase [45], whereas along with the cubic phase $ZrO_2(8Y)$ can also have inclusions of a tetragonal phase [46]. It can result in concentration of an electric field in a region of grains with the different structure [47], which, in turn, results in localization of the filament and reduction of the spread of the current states.

Fig. 6 shows the current-voltage curves of the $ZrO_2(12Y)$-based memristor stacks with the electrodes made of the different chemically active metals (Ta, W and Ru), which are measured at the same value of I_{CC}, which is 1 mA and corresponds to the minimum value of I_{CC}, at which the stacks with the W or Ru electrode demonstrate resistive switching.

The stacks with the Ta and W electrode demonstrate close resistive switching parameters (currents and switching voltages) which are compatible with CMOS-integration

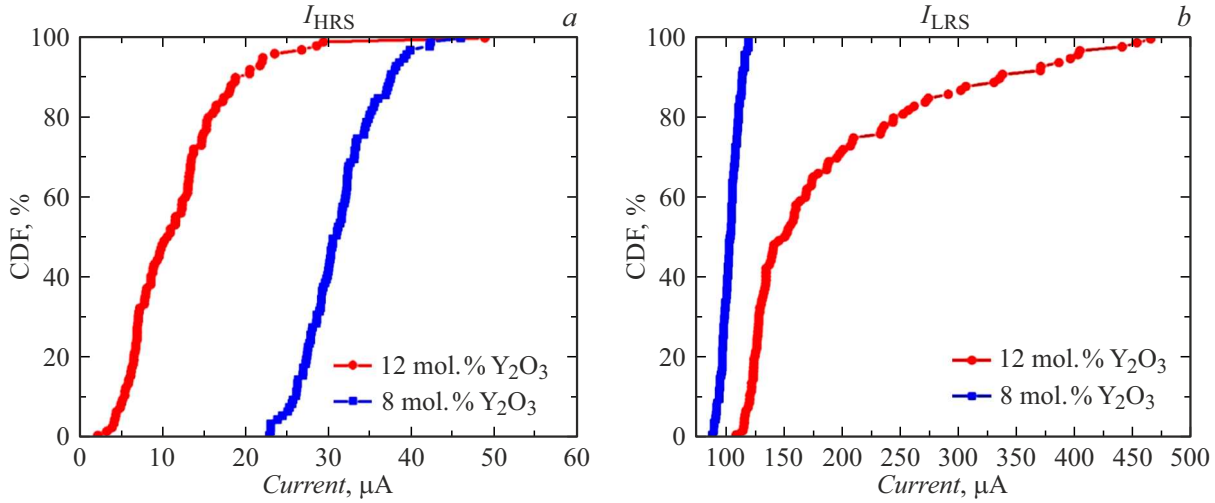

Figure 5. Cumulative distribution functions (CDF) of I_{HRS} (*a*) and I_{LRS} (*b*), which are obtained from the current-voltage curves shown in Fig. 4, at the read-out voltage of +0.15 V.

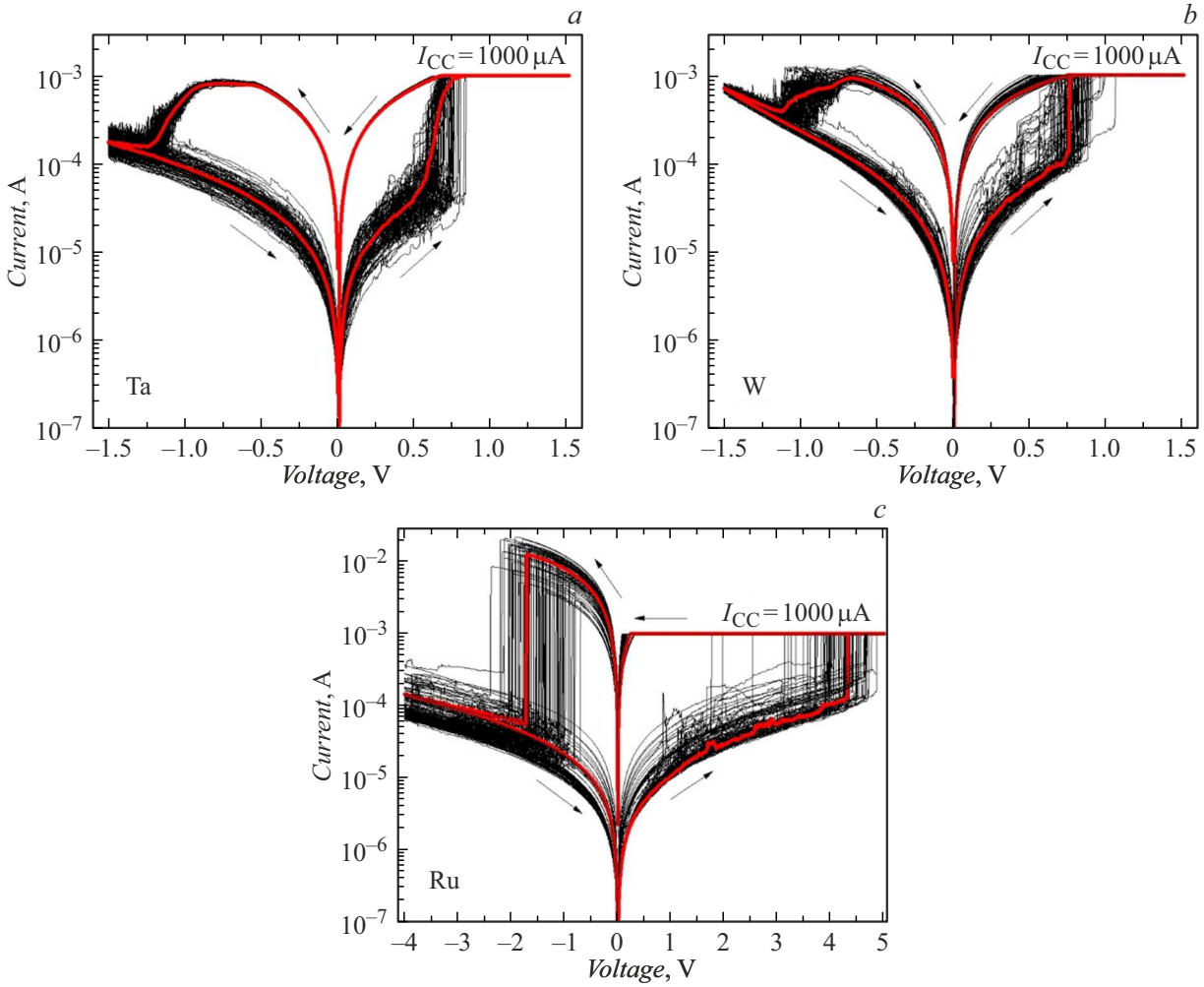

Figure 6. Typical current-voltage curves of the ZrO_2(12Y)-based stacks with the electrodes made of different chemically active metals: Ta (*a*), W (*b*) and Ru (*c*). The graphs show series of 100 current-voltage characteristics (in black) and the averaged curves (in red).

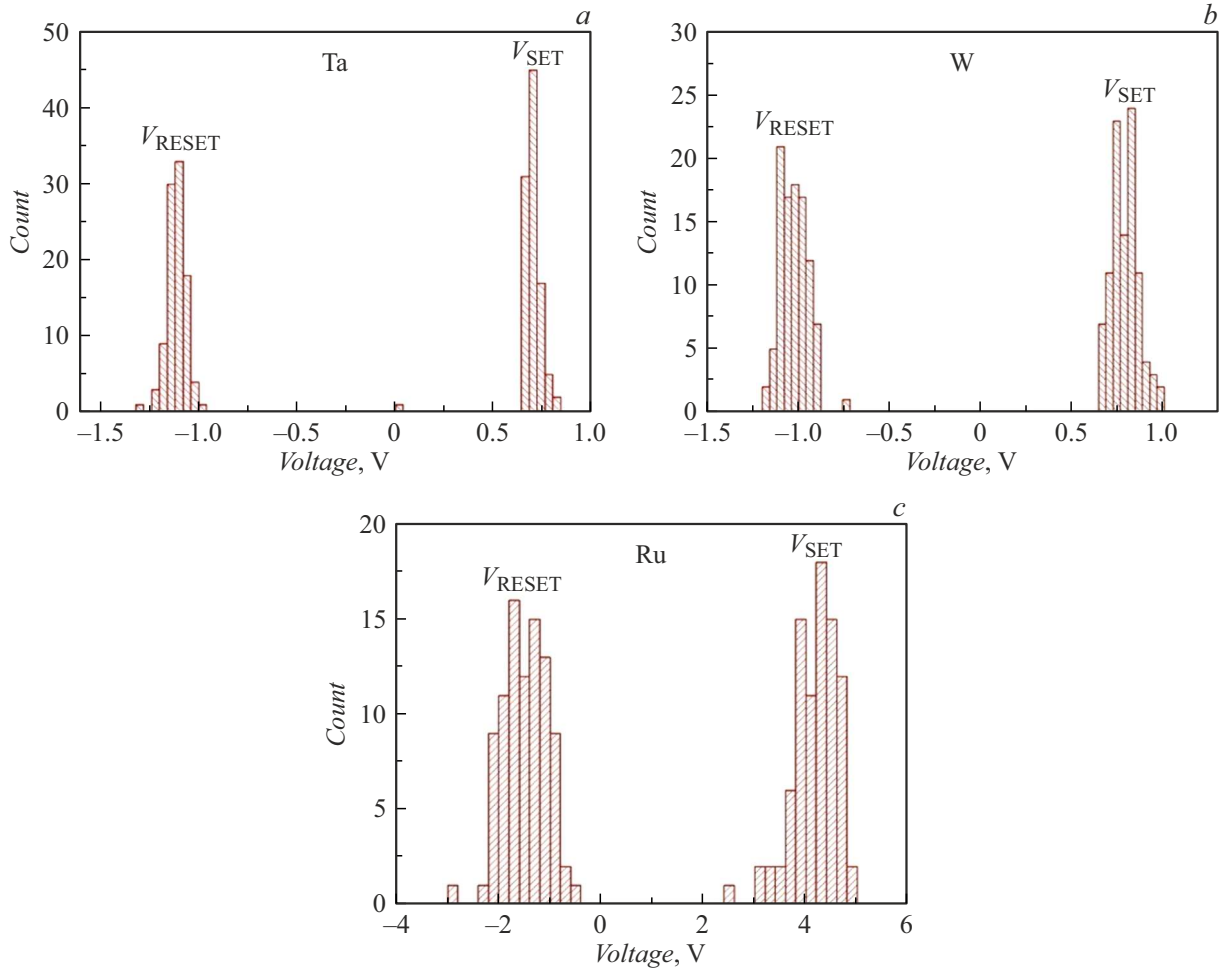

Figure 7. Histograms of distributions of V_{SET} and V_{RESET}, as obtained from the current-voltage curves of Fig. 6, for the ZrO_2(12Y)-based stacks with the electrodes made of the different chemically active metals: Ta (*a*), W (*b*) and Ru (*c*).

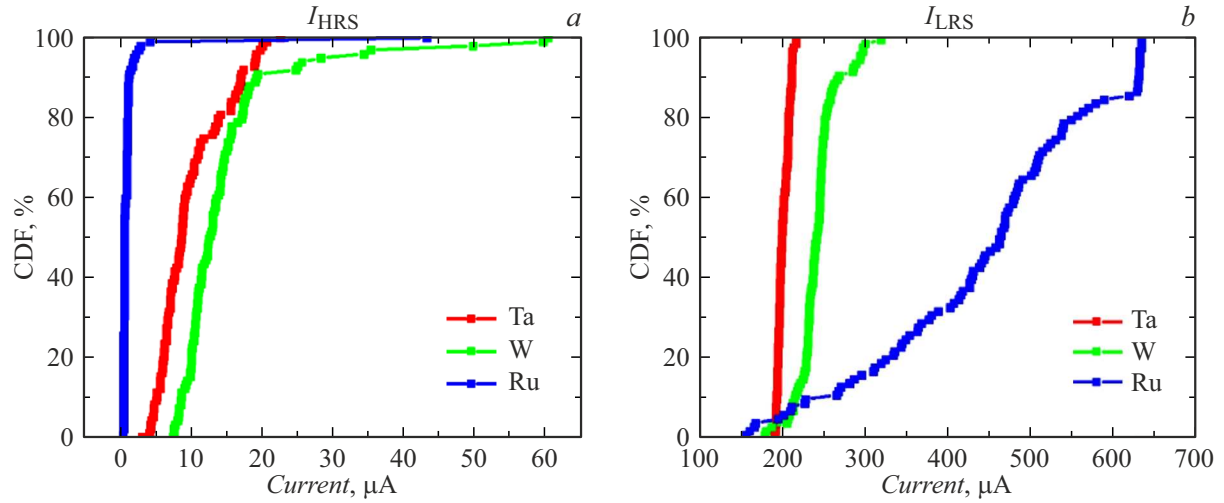

Figure 8. Cumulative distribution functions (CDF) of I_{HRS} (*a*) and I_{LRS} (*b*), which are obtained from the current-voltage curves shown in Fig. 6, at the read-out voltage of +0.15 V.

requirements. In terms of stability of the switching parameters, the best characteristics belong to the stacks with the Ta electrode (Fig. 6, *a*); moreover, they start operating at significantly smaller limitation currents, thereby potentially

meaning smaller energy consumption of these memristors. The stacks with W as the upper active electrode (Fig. 6, *b*) demonstrate less stable resistive switchings — they have a larger spread of both the switching voltages (Fig. 7) and the current states (Fig. 8).

The stacks with Ru as the upper electrode demonstrate the worst characteristics. The switchings are realized only at high limitation currents 1–2 mA and occur at high voltages ±5 V. The spread of the current states is the largest among all the used materials of the active electrode. At the same time, the maximum currents achievable in the RESET process can exceed the values of 10 mA, which is incompatible with the CMOS requirements.

The observed effect of the electrode material on the resistive switching parameters is related to variation of oxygen exchange in the resistive switching area and can be qualitatively explained by a difference of the values of $\Delta_f G^o$ (see Table). The value of $\Delta_f G^o$ for Ru is close to zero, therefore, it can absorb only a small number of the oxygen ions. Therefore, formation of the filament in the ZrO_2(12Y) film requires high voltage, which is why a large spread of the resistive switching parameters is observed (Fig. 6, *c*). The value of $\Delta_f G^o$ for Ta or W is comparable to that for Zr, that is why the Ta or W electrode in the resistive switching process serves as an effective container for oxygen ions. Therefore, oxidation-reduction processes are realized at smaller voltages, while the resistive switchings occur with preservation of a main part of the filament, thereby contributing to the significantly smaller spread of the resistive switching parameters.

Standard free energy of formation of the metal oxide (the standard formation Gibbs energy formation $\Delta_f G^o$) as calculated per O_2 [38]

	RuO_4	WO_2	Ta_2O_5	ZrO_2
$\Delta_f G^o$, kJ/mol	−75	−533	−778	−1100

Conclusion

It is shown in the present study for the memristor stacks based on stabilized zirconium dioxide that the resistive switching parameters (currents in the various resistive states and their spread, switching voltages, etc.) can be monitored by controllably changing the concentration of the oxygen vacancies, especially in the resistive switching area, — a local area between a tip of the filament and one of the electrode, by varying the concentration of the ZrO_2 dopant (8 and 12 mol.% of Y_2O_3) or changing the oxygen exchange parameters due to using the different electrode materials (for example, Ta, W or Ru).

In particular, it is found by the XPS method that the metal electrodes made of Ta and W oxidize during formation of the ZrO_2(Y)-based memristor stacks with generation of TaO_2, Ta_2O_5 and W_2O_3. As a result, the insulator/electrode interface has an area saturated with the oxygen vacancies formed. Due to quite large equilibrium concentration of the oxygen vacancies, which is formed due to doping zirconium dioxide with yttrium oxide, in the initial state (before the electrophysical measurements) the ZrO_2(Y) layer has conducting channels formed, along which electron conductivity is realized. Locations where these channels go out to the ZrO_2(Y) surface are recorded by the conducting AFM method.

It is shown that the stacks produced using the smaller concentration of the dopant demonstrate smooth resistive switching and the smaller current ratio in the resistive states and can be interesting for neuromorphic applications. The stacks with the Ta electrode demonstrate the CMOS-compatible values of currents and switching voltages as well as the least spread of these parameters. At the same time, the stacks with the W electrode demonstrate the similar resistive switching parameters, but a larger spread thereof. The stacks with the Ru electrode have the worst resistive switching parameters (high values of the resistive switching voltages and the currents as well as their significant spread), which are incompatible with the CMOS requirements.

Thus, correct selection of materials of the insulator and the electrodes is a key to successful integration of the memristor devices into the standard CMOS process and to subsequent wide introduction of the memristors into microelectronic products.

The obtained results can be recommended to be used when designing and developing the memristor devices with reproducible electrophysical characteristics for creating CMOS-compatible nonvolatile elements of resistive memory and neuromorphic applications.

Funding

The study was carried out under the state assignment № FSWR-2025-0006 (Research Laboratory „Memristor Nanoelectronics Laboratory“).

Acknowledgments

The studies were conducted using the equipment of the Center for Collective Use of the Scientific and Educational Center „Physics of Solid-State Nanostructures“ and the Educational Design Center of Electronics of Lobachevsky State University of Nizhny Novgorod.

Conflict of interest

The authors declare that they have no conflict of interest.

References

[1] A.N. Mikhaylov, E.G. Gryaznov, M.N. Koryazhkina, I.A. Bordanov, S.A. Shchanikov, O.A. Telminov, V.B. Kazantsev. Supercomp. Frontiers and Innovations, **10** (2), 77 (2023). DOI: 10.14529/jsfi230206

[2] X. Duan, Z. Cao, K. Gao, W. Yan, S. Sun, G. Zhou, Z. Wu, F. Ren, B. Sun. Adv. Mater., **36** (14), 2310704 (2024). DOI: 10.1002/adma.202310704
[3] M. Lanza, R. Waser, D. Ielmini, J.J. Yang, L. Goux, J. Suñe, A.J. Kenyon, A. Mehonic, S. Spiga, V. Rana, S. Wiefels, S. Menzel, I. Valov, M.A. Villena, E. Miranda, X. Jing, F. Campabadal, M.B. Gonzalez, F. Aguirre, F. Palumbo, K. Zhu, J.B. Roldan, F.M. Puglisi, L. Larcher, T.-H. Hou, T. Prodromakis, Y. Yang, P. Huang, T. Wan, Y. Chai, K.L. Pey, N. Raghavan, S. Dueñas, T. Wang, Q. Xia, S. Pazos. ACS Nano, **15** (11), 17214 (2021). DOI: 10.1021/acsnano.1c06980
[4] O. Kapur, D. Guo, J. Reynolds, D. Newbrook, Y. Han, R. Beanland, L. Jiang, C.H. Kees de Groot, R. Huang. Sci. Reports, **14**, 14008 (2024). DOI:10.1038/s41598-024-64499-2
[5] F. Cai, J.M. Correll, S.H. Lee, Y. Lim, V. Bothra, Z. Zhang, M.P. Flynn, W.D. Lu. Nature Electron., **2**, 290 (2019). DOI: 10.1038/s41928-019-0270-x
[6] M. Rao, H. Tang, J. Wu, W. Song, M. Zhang, W. Yin, Y. Zhuo, F. Kiani, B. Chen, X. Jiang, H. Liu, H.-Y. Chen, R. Midya, F. Ye, H. Jiang, Z. Wang, M. Wu, M. Hu, H. Wang, Q. Xia, N. Ge, J. Li, J.J. Yang. Nature, **615**, 823 (2023). DOI: 10.1038/s41586-023-05759-5
[7] J.S. Lee, S. Lee, T.W. Noh. Appl. Phys. Rev., **2** (3), 031303 (2015). DOI: 10.1063/1.4929512
[8] B. Mohammad, M.A. Jaoude, V. Kumar, D.M. Al Homouz, H.A. Nahla, M. Al-Qutayri, N. Christoforou. Nanotechnol. Rev., **5** (3), 311 (2016). DOI: 10.1515/ntrev-2015-0029
[9] R. Waser. J. Nanosci. Nanotechnol., **12** (10), 7628 (2012). DOI: 10.1166/jnn.2012.6652
[10] D. Ielmini. Semicond. Sci. Technol., **31** (6), 063002 (2016). DOI: 10.1088/0268-1242/31/6/063002
[11] A. Kindsmüller, A. Meledin, J. Mayer, R. Waser, D. Wouters. Nanoscale, **11** (39), 18201 (2019). DOI: 10.1039/c9nr06624a
[12] S.-Y. Wang, D.-Y. Lee, T.-Y. Tseng, C.-Y. Lin. Appl. Phys. Lett., **95**, 112904 (2009). DOI: 10.1063/1.3231872
[13] N.K. Upadhyay, W. Sun, P. Lin, S. Joshi, R. Midya, X. Zhang, Z. Wang, H. Jiang, J.H. Yoon, M. Rao, M. Chi, Q. Xia, J.J. Yang. Adv. Electron. Mater., **6** (5), 1901411 (2020). DOI: 10.1002/aelm.201901411
[14] H. Zhang, B. Gao, B. Sun, G. Chen, L. Zeng, L. Liu, X. Liu, J. Lu, R. Han, J. Kang, B. Yu. Appl. Phys. Lett., **96** (12), 123502 (2010). DOI: 10.1063/1.3364130
[15] A.V. Kruglov, D.A. Serov, A.I. Belov, M.N. Koryazhkina, I.N. Antonov, S.Yu. Zubkov, R.N. Kryukov, A.N. Mikhailov, D.O. Filatov, O.N. Gorshkov. ZhTF, **94** (11), 1833 (2024) (in Russian). DOI: 10.61011/JTF.2024.11.59100.204-24
[16] H.A. Abbas. *Stabilized Zirconia for Solid Oxide Fuel Cells or Oxygen Sensors: Characterization of Structural and Electrical Properties of Zirconia Doped with Some Oxides* (LAP LAMBERT Academic Publishing, Saarbrucken, 2012)
[17] M. Filal, C. Petot, M. Mokchah, C. Chateau, J.L. Carpentier. Solid State Ionics, **80** (1–2), 27 (1995). DOI: 10.1016/0167-2738(95)00137-U
[18] T. Liu, X. Zhang, X. Wang, J. Yu, L. Li. Ionics, **22**, 2249 (2016). DOI: 10.1007/s11581-016-1880-1
[19] A. Bogicevic, C. Wolverton, G.M. Crosbie, E.B. Stechel. Phys. Rev. B, **64** (1), 014106 (2001). DOI: 10.1103/PhysRevB.64.014106
[20] V.G. Zavodinskii. FTT, **46** (3), 441 (2004) (in Russian).
[21] R. Devanathan, W.J. Weber, S.C. Singhal, J.D. Gale. Solid State Ionics, **177** (15–16), 1251 (2006). DOI: 10.1016/j.ssi.2006.06.030
[22] R. Krishnamurthy, Y.-G. Yoon, D.J. Srolovitz, R. Car. J. American Ceramic Society, **87** (10), 1821 (2004). DOI: 10.1111/j.1151-2916.2004.tb06325.x
[23] S. Tikhov, O. Gorshkov, I. Antonov, A. Morozov, M. Koryazhkina, D. Filatov. Adv. Condens. Matter Phys., **2018** (8), 2028491 (2018). DOI: 10.1155/2018/2028491
[24] A.V. Yakimov, D.O. Filatov, O.N. Gorshkov, D.A. Antonov, D.A. Liskin, I.N. Antonov, A.V. Belyakov, A.V. Klyuev, A. Carollo, B. Spagnolo. Appl. Phys. Lett., **114** (25), 253506 (2019). DOI: 10.1063/1.5098066
[25] J. Yang, J. Strachan, F. Miao, M.-X. Zhang, M. Pickett, W. Yi, D. Ohlberg, G. Medeiros-Ribeiro, R. Williams. Appl. Phys. A, **102** (4), 785 (2011). DOI: 10.1007/s00339-011-6265-8
[26] C. Chen, S. Gao, F. Zeng, G.S. Tang, S.Z. Li, C. Song, H.D. Fu, F. Pan. J. Appl. Phys., **114** (1), 014502 (2013). DOI: 10.1063/1.4812486
[27] N. Ge, M.-X. Zhang, L. Zhang, J. Yang, Z. Li, R. Williams. Semicond. Sci. Technol., **29** (10), 104003 (2014). DOI: 10.1088/0268-1242/29/10/104003
[28] C.-Y. Lin, C. Wu, C.-Y. Wu, T.-C. Lee, F.-L. Yang, C. Hu, T. Tseng. IEEE Electron Device Lett., **28** (5), 366 (2007). DOI: 10.1109/LED.2007.894652
[29] S.Yu. Zubkov, I.N. Antonov, O.N. Gorshkov, A.P. Kasatkin, R.N. Kryukov, D.E. Nikolichev, D.A. Pavlov, M.E. Shenina. FTT, **60** (3), 591 (2018) (in Russian). DOI: 10.21883/FTT.2018.03.45566.249
[30] F. Iacona, R. Kelly, G. Marletta. J. Vacuum Sci. Technol. A, **17** (5), 2771 (1999). DOI: 10.1116/1.581943
[31] M.-S. Kim, Y.-D. Ko, J.-H. Hong, M.-C. Jeong, J.-M. Myoung, I. Yun. Appl. Surf. Sci., **227** (1–4), 387 (2004). DOI: 10.1016/j.apsusc.2003.12.017
[32] B.J. Choi, D.S. Jeong, S.K. Kim. J. Appl. Phys., **98** (3), 033715 (2005). DOI: 10.1063/1.2001146
[33] B. Singh, B.R. Mehta, D. Varandani, A.V. Savu, J. Brugger. Nanotechnology, **23** (49), 495707 (2012). DOI: 10.1088/0957-4484/23/49/495707
[34] V. Iglesias, M. Lanza, A. Bayerl, M. Porti, M. Nafría, X. Aymerich, L.F. Liu, J.F. Kang, G. Bersuker, K. Zhang, Z.Y. Shen. Microelectron. Reliability, **52** (9–10), 2110 (2012). DOI: 10.1016/j.microrel.2012.06.073
[35] M. Setvin, M. Reticcioli, F. Poelzleitner, J. Hulva, M. Schmid, L.A. Boatner, C. Franchini, U. Diebold. Science, **359** (6375), 572 (2018). DOI: 10.1126/science.aar2287
[36] K. Kukl, J. Aarik, A. Aidla, O. Kohan, T. Uustare, V. Sammelselg. Appl. Surf. Sci., **230** (1), 249 (2004). DOI: 10.1016/j.apsusc.2004.02.033
[37] P.A. Murawala, M. Sawai, T. Tatsuta, O. Tsuji, S. Fujita, S. Fujita. Jpn. J. Appl. Phys., **32** (1S), 368 (1993). DOI: 10.1143/JJAP.32.368
[38] D.R. Lide. *CRC Handbook of Chemistry and Physics* (CRC Press, Boca Raton, 2016)
[39] Z. Wang, H. Jiang, M.H. Jang, P. Lin, A. Ribbe, Q. Xia, J.J. Yang. Nanoscale, **8** (29), 14023 (2016). DOI: 10.1039/C6NR01085G

[40] A.N. Mikhaylov, E.G. Gryaznov, A.I. Belov, D.S. Korolev, A.N. Sharapov, D.V. Guseinov, D.I. Tetelbaum, S.V. Tikhov, N.V. Malekhonova, A.I. Bobrov, D.A. Pavlov, S.A. Gerasimova, V.B. Kazantsev, N.V. Agudov, A.A. Dubkov, C.M.M. Rosário, N.A. Sobolev, B. Spagnolo. Phys. Status Solidi C, **13** (10–12), 8701 (2016). DOI: 10.1002/pssc.201600083
[41] A.A. Koroleva, A.G. Chernikova, A.A. Chouprik, E.S. Gornev, A.S. Slavich, R.R. Khakimov, E.V. Korostylev, C.S. Hwang, A.M. Markeev. ACS Appl. Mater. Interfaces, **12** (49), 55331 (2020). DOI: 10.1021/acsami.0c14810
[42] M. Lanza, K. Zhang, M. Porti, M. Nafría, Z.Y. Shen, L.F. Liu, J.F. Kang, D. Gilmer, G. Bersuker. Appl. Phys. Lett., **100** (12), 123508 (2012). DOI: 10.1063/1.3697648.
[43] M. Lanza, G. Bersuker, M. Porti, E. Miranda, M. Nafría, X. Aymerich. Appl. Phys. Lett., **101** (19), 193502 (2012). DOI: 10.1063/1.4765342.
[44] D. Yang, J. Xue, J. Wang, H. Wang, S. Wang, X. Lei, J. Yan, W. Zhao. ACS Appl. Electron. Mater., **6** (6), 4764 (2024). DOI: 10.1021/acsaelm.4c00790
[45] Yu.S. Kuz'minov, E.E. Lomonova, V.V. Osiko. *Tugoplavkie materialy iz kholodnogo tiglya* (Nauka, M., 2004) (in Russian).
[46] R. Frison, S. Heiroth, J.L.M. Rupp, K. Conder, E.J. Barthazy, E. Müller, M. Horisberger, M. Döbeli, L.J. Gauckler. Solid State Ionics, **232**, 29 (2013). DOI: 10.1016/j.ssi.2012.11.014
[47] B.K. You, W.I. Park, J.M. Kim, K.-I. Park, H.K. Seo, J.Y. Lee, Y.S. Jung, K.J. Lee. ACS Nano, **8** (9), 9492 (2014). DOI: 10.1021/nn503713f

Translated by M.Shevelev